arXiv:1607.04516v1 [cond-mat.mes-hall] 15 Jul 2016

Exploiting vibrational strong coupling to make an optical parametric oscillator out of a Raman laser

Javier del Pino,[1] Francisco J. Garcia-Vidal,[1,2,*] and Johannes Feist[1,†]

[1] *Departamento de Física Teórica de la Materia Condensada and Condensed Matter Physics Center (IFIMAC), Universidad Autónoma de Madrid, E-28049 Madrid, Spain*

[2] *Donostia International Physics Center (DIPC), E-20018 Donostia/San Sebastián, Spain*

When the collective coupling of the rovibrational states in organic molecules and confined electromagnetic modes is sufficiently strong, the system enters into vibrational strong coupling, leading to the formation of hybrid light-matter quasiparticles. In this work we demonstrate theoretically how this hybridization in combination with stimulated Raman scattering can be utilized to widen the capabilities of Raman laser devices. We explore the conditions under which the lasing threshold can be diminished and the system can be transformed into an optical parametric oscillator. Finally, we show how the dramatic reduction of the many final molecular states into two collective excitations can be used to create an all-optical switch with output in the mid-infrared.

PACS numbers: 71.36.+c, 42.55.Ye, 42.65.Yj, 42.50.Nn, 78.66.Qn

When the coherent interaction between a confined light mode and vibrational matter excitations becomes faster than the relevant decoherence processes, the system can enter into vibrational strong coupling (VSC) [1–6]. The fundamental excitations of the two systems then become inextricably linked and can be described as hybrid light-matter quasiparticles, so-called vibro-polaritons, that combine the properties of both ingredients. In particular, the use of vibrational modes that are both IR- and Raman-active allows to probe vibro-polaritons through Raman scattering mediated by their material component [7–9].

On the other hand, while the cross sections for Raman scattering are typically small, the process can become highly efficient under strong driving if the scattered Stokes photons accumulate sufficiently to lead to stimulated Raman scattering (SRS) [10]. The effective energy conversion from input to output beam can then be exploited to fabricate a highly tunable Raman laser. Raman lasers have been realized using a variety of nonlinear media and configurations, such as under pulsed operation in optical fibers [11], nonlinear crystals [12], gases [13], or silicon [14], as well as under continuous-wave operation in silicon [15, 16], silica [17] and molecular hydrogen [18]. Since the threshold powers for these systems are typically large, they suffer from detrimental effects such as Kerr nonlinearities, four-wave mixing, and heat deposition [12].

In this Letter, we propose and theoretically demonstrate that the hybrid light-matter nature of vibro-polaritons can be exploited to obtain photon emission from the vibrationally excited final states of a Raman laser. A single-output Raman laser device then becomes analogous to an *optical parametric oscillator* (OPO) [19] with output beams both in the visible and in the mid-IR, relevant for many spectroscopic applications [20]. In addition to obtaining two coherent beams with a stable phase relation (and possibly nonclassical correlations [21–23]) spanning very different frequency regions, this approach has the further advantage of effectively getting rid of the energy deposited into material vibrations; instead of being dissipated as heat, this energy is emitted in the form of photons. Finally, we show that the coexistence of the upper and lower polariton modes with very similar properties can be exploited to produce an all-optical switch [24, 25]. Here, one (gate) pump beam can be used to switch Raman lasing of a second (signal) pump beam.

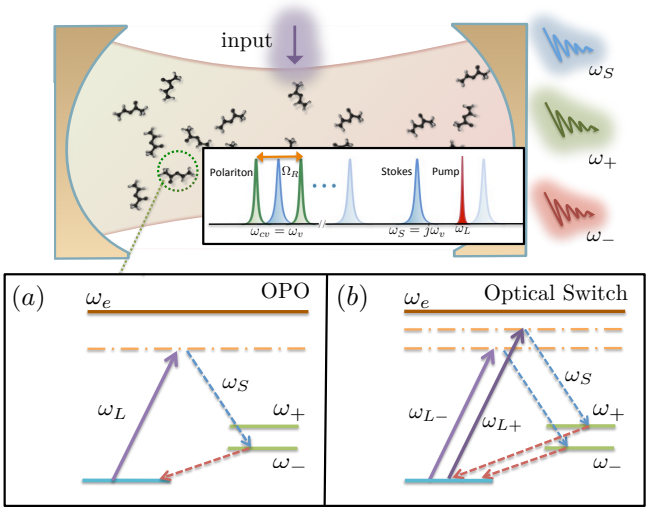

FIG. 1. Upper panel: sketch of the system to convert a Raman laser into an OPO through vibrational strong coupling (see main text). The input fields (purple arrows) can be chosen to achieve (a) OPO operation with a single pump frequency ω_L, or (b) an all-optical switch with two pump fields $\omega_{L\pm}$.

The system we consider (sketched in Fig. 1) consists of a material with a vibrational transition that is both IR- and Raman-active, placed inside a resonator (e.g., a microcavity). The resonator supports at least two confined modes, a mid-IR mode used to achieve VSC with

* fj.garcia@uam.es
† johannes.feist@uam.es

the vibrational transition, and an optical mode used to accumulate the scattered Stokes photons. We model the material as a set of N noninteracting three-level quantum emitters, formed by the ground state $|g\rangle$ (energy $\omega_g \equiv 0$), the first excited vibrational mode $|v\rangle$ (energy ω_v), and an electronically excited state $|e\rangle$ (energy ω_e) [8]. While this model can naturally represent organic molecules (as used in current experiments achieving VSC), we note that it can also be used to treat systems such as the nonlinear crystals utilized in existing Raman lasers. The IR-active ground-vibrational transition is resonantly coupled to the mid-IR cavity mode at frequency ω_c, with annihilation operator $\hat{a}_c$. The Hamiltonian describing the vibrational excitations and their strong coupling to the mid-IR mode within the rotating wave approximation (RWA) is given by (setting $\hbar = 1$ here and in the following)

$$\hat{H}_s = \omega_c \hat{a}_c^\dagger \hat{a}_c + \sum_{i=1}^{N} \left[\omega_v \hat{\sigma}_{vv}^{(i)} + \left(g \hat{a}_c^\dagger \hat{\sigma}_{gv}^{(i)} + \text{H.c.} \right) \right]. \quad (1)$$

Here, $\hat{\sigma}_{ab}^{(i)} = |a^{(i)}\rangle\langle b^{(i)}|$ denotes the transition operator between the states $|b\rangle$ and $|a\rangle$ of the ith molecule, while the light-matter interaction strength is measured by g, which depends on the single-photon electric field strength of the mid-IR cavity mode and the change of the molecular dipole moment under displacement from the equilibrium position.

Assuming zero detuning ($\omega_c = \omega_v$) for simplicity, the eigenstates of $\hat{H}_s$ are formed by *i)* two vibro-polaritons, $|\pm\rangle = \frac{1}{\sqrt{2}}(\hat{a}_c^\dagger|G\rangle \pm |B\rangle)$, symmetric and antisymmetric hybridizations of the cavity mode with the collective *bright state* of the molecular vibrations, $|B\rangle = \frac{1}{\sqrt{N}} \sum_{i=1}^{N} |v^{(i)}\rangle$. Here, $|G\rangle$ denotes the global ground state. The polaritons have eigenfrequencies $\omega_\pm = \omega_v \pm g\sqrt{N}$, separated by the Rabi splitting $\Omega_R = 2g\sqrt{N}$. The other eigenstates are *ii)* $N-1$ so-called *dark states* $|d\rangle$ orthogonal to $|B\rangle$ that have eigenfrequencies ω_v and no electromagnetic component.

We first treat the dynamics of the system under external driving of a single pump mode at frequency ω_L (not resonant with any cavity mode), see Fig. 1(a). The full Hamiltonian then contains $\hat{H}_s$ as well as the electronic excitations of the molecules, the pump field (which we quantize in order to be able to describe depletion [26]), the cavity mode in the optical (frequency ω_S), and the interactions between the molecular transitions and the optical modes, leading to

$$\hat{H} = \hat{H}_s + \omega_S \hat{n}_S + \omega_L \hat{n}_L + \sum_{i=1}^{N} \left[\omega_e \hat{\sigma}_{ee}^{(i)} + \left(g_S \hat{a}_S \hat{\sigma}_{ve}^{(i)\dagger} + g_L \hat{a}_L \hat{\sigma}_{ge}^{(i)\dagger} + \text{H.c.} \right) \right], \quad (2)$$

where $\hat{n}_L = \hat{a}_L^\dagger \hat{a}_L$ and $\hat{n}_S = \hat{a}_S^\dagger \hat{a}_S$ are the photon number operators for the pump laser and confined cavity mode, which are coupled (within the RWA) to the ground-excited and excited-vibrational transitions in the molecules, respectively. We assume continuous-wave driving of the pump mode,

$$\hat{H}_d = \Phi_{\text{in}} \sqrt{\kappa_L} (\hat{a}_L e^{-i\omega_L t} + \hat{a}_L^\dagger e^{i\omega_L t}), \quad (3)$$

where Φ_{in} parametrizes the driving strength. The results derived below are also valid under time-dependent driving as long as the pump amplitude Φ_{in} varies more slowly than the time required to reach the steady state.

When the driving laser is far off-resonant to the electronic transition such that the hierarchy condition $\omega_e \gg \omega_L \gg \omega_v$ is satisfied, we can adiabatically eliminate the electronically excited states from the problem [27, 28]. If the laser frequency is chosen such that Raman scattering to one of the polaritonic modes is resonant with cavity mode S, i.e., $\omega_L = \omega_S + \omega_p$, with $p \in \{+, -\}$, scattering to the other polaritonic mode can then be neglected under a second RWA. This gives the following effective Hamiltonian (for details see the supplemental material [29]):

$$\hat{H}_{\text{eff}} \simeq \omega_L \hat{n}_L + \omega_S \hat{n}_S + \omega_p \hat{\sigma}_{pp} - g_{\text{eff}}^p \left(\hat{a}_L \hat{a}_S^\dagger \hat{\sigma}_{Gp}^\dagger + \text{H.c.} \right), \quad (4)$$

where the effective coupling occurs between laser photons and pairs of Stokes photons and polaritons, while the dark modes are not excited. The coupling strength is given by

$$g_{\text{eff}}^p = \sqrt{\frac{N}{2}} \frac{g_S g_L}{\omega_e - (\omega_p + \omega_S)}, \quad (5)$$

and is not sensitive to the Rabi splitting of the polaritons. This agrees with the case of linear Raman scattering, where theory predicts a redistribution of the scattering cross section of the system without further enhancement [8, 9]. When deriving g_{eff}^p, we have assumed perfect spatial overlap between the three involved modes L, S, and p; inclusion of the spatial profile would lead to the renormalization $g_{\text{eff}}^\eta \to g_{\text{eff}}^\eta \mathcal{S}$, with $\mathcal{S}$ the overlap integral.

The trilinear interaction in Eq. (4) is analogous to a nondegenerate OPO, converting an input laser beam into two new modes, the "signal" (Stokes beam) and "idler" (vibrations) [19]. While this analogy is well-known [10], it is merely formal for a standard Raman laser (i.e., in the weak-coupling regime) since most of the excitation in the vibrationally excited states decays nonradiatively, such that no idler beam is emitted. In the VSC regime, however, the hybrid light-matter nature of the polariton imbues them with a photonic component, leading to efficient outcoupling in the form of photons. This makes the analogy complete and provides an approach towards converting a Raman laser into an OPO.

We next discuss the role of losses and dephasing. Within the standard Lindblad master-equation formalism, the density operator $\hat{\rho}$ evolves according to

$$\partial_t \hat{\rho} = -i[\hat{H}_{\text{eff}}, \hat{\rho}] + \kappa_S \mathcal{L}_{\hat{a}_S}[\hat{\rho}] + \kappa_L \mathcal{L}_{\hat{a}_L}[\hat{\rho}] + \tilde{\Gamma}_{\text{vib}}[\hat{\rho}], \quad (6)$$

where $\mathcal{L}_X[\hat{\rho}] = \hat{X}\hat{\rho}\hat{X}^\dagger - \frac{1}{2}\{\hat{X}^\dagger\hat{X}, \hat{\rho}\}$. The loss rates of the Stokes and quantized laser modes are given by κ_S and κ_L,

respectively. The term $\tilde{\Gamma}_{\rm vib}$ summarizes all decoherence mechanisms affecting the vibrationally excited subspace. Under weak coupling, these consist of nonradiative decay ($\gamma_v \mathcal{L}_{\hat{\sigma}_{gv}}$) and pure dephasing ($\gamma_\varphi \mathcal{L}_{\hat{\sigma}_{vv}}$). In the VSC regime, the influence of inhomogeneous broadening and dephasing can be suppressed for large enough Rabi splitting [4, 30], leading to an effective decay of the polaritons ($\Gamma_\pm \mathcal{L}_{\hat{\sigma}_{g\pm}}$) with a rate as small as $\Gamma_\pm \approx \frac{\kappa_c+\gamma_v}{2}$, significantly below the average of the bare-molecule ($\gamma_v+\gamma_\varphi$) and mid-IR cavity (κ_c) linewidths.

In order to characterize the threshold condition and quantum yield of the VSC-based OPO described above, we calculate the steady-state mode populations within the mean-field-approximation, in which all fields are assumed to be described by coherent amplitudes. In terms of the slowly-varying amplitudes $\alpha_L = \langle \hat{a}_L \rangle e^{i\omega_L t}$, $\alpha_S = \langle \hat{a}_S \rangle e^{i\omega_S t}$, and $\psi_p = \langle \hat{\sigma}_{Gp} \rangle e^{i\omega_p t}$, the semi-classical Heisenberg-Langevin equations of motion become

$$\partial_t \alpha_L = i g^p_{\rm eff} \psi_p \alpha_S - \kappa_L \alpha_L + i\sqrt{\kappa_L}\Phi_{\rm in}, \tag{7a}$$
$$\partial_t \alpha_S = i g^p_{\rm eff} \psi_p^* \alpha_L - \kappa_S \alpha_S, \tag{7b}$$
$$\partial_t \psi_p = i g^p_{\rm eff} \alpha_S^* \alpha_L - \Gamma_p \psi_p. \tag{7c}$$

The corresponding steady-state solutions (which agree with the classical treatment of an OPO [31]) can be parametrized in terms of $f = \Phi_{\rm in}/\Phi_{\rm th}$, where $\Phi_{\rm th} = \sqrt{\kappa_L \kappa_S \Gamma_p}/g^p_{\rm eff}$ is the threshold value for the driving parameter. Below threshold ($f<1$), neither the polariton nor the Stokes mode are populated ($|\psi_p|^2 = |\alpha_S|^2 = 0$), while the pump mode has population $|\alpha_L|^2 = f^2\Phi^2_{\rm th}/\kappa_L$. Above threshold ($f \geq 1$), the pump amplitude becomes independent of the driving power (so-called pump clamping), $|\alpha_L|^2 = \Phi^2_{\rm th}/\kappa_L$, while the Stokes and polariton mode occupations grow linearly with input power, $|\psi_p|^2 = (f-1)\Phi^2_{\rm th}/\Gamma_p$ and $|\alpha_S|^2 = (f-1)\Phi^2_{\rm th}/\kappa_S$. This implies that the conversion efficiency approaches 100% if the pumping is sufficiently strong. Explicitly, the quantum yield for conversion of input photons to pairs of Stokes photons and polaritons follows the simple relation

$$\mathcal{Q} = \frac{P_S/\omega_S}{P_{\rm in}/\omega_L} = 1 - \frac{1}{f}, \tag{8}$$

where $P_S/\omega_S = \kappa_S|\alpha_S|^2$ ($= P_p/\omega_p$) is the flux of emitted Stokes photons, and $P_{\rm in} = \omega_L \Phi_{\rm in}\Phi_{\rm th}$ is the input power.

The number of photons emitted at the vibro-polariton frequency (typically in the mid-IR [1]) is equal to the number of generated Stokes photons, multiplied by the radiative emission efficiency of the polaritons, $\beta = \Gamma_p^{\rm rad}/\Gamma_p$. For zero detuning and a mid-IR cavity without nonradiative losses (such as a dielectric cavity [6]), this is given by $\beta = \frac{\kappa_c}{\kappa_c+\gamma_v}$, which is close to unity for the experimentally relevant regime $\kappa_c \gg \gamma_v$. In a standard Raman laser, the energy deposited into the vibrational modes is converted to heat, limiting the achievable powers [12, 19]. In contrast, the vibro-polariton Raman OPO proposed here converts this energy efficiently into an additional coherent output beam at mid-IR frequencies, and thus simultaneously reduces heating significantly.

Furthermore, the ratio between the thresholds for polariton-based OPO operation under strong coupling and for the bare-molecule Raman laser under weak coupling is given by

$$\frac{\Phi^{SC}_{\rm th}}{\Phi^{WC}_{\rm th}} = \sqrt{\frac{\Gamma_p}{\gamma_v+\gamma_\varphi}} \approx \sqrt{\frac{\kappa_c}{2\gamma_\varphi}}. \tag{9}$$

This demonstrates that for the common case that the inhomogeneous width and dephasing of the vibrational modes are faster than the cavity losses ($\gamma_\varphi > \kappa_c$), the vibro-polariton Raman OPO has a lower threshold power than the equivalent Raman laser. In addition, depending on the relative lifetimes of the vibro-polaritons Γ_p and the Stokes photons κ_S, there can be significant accumulation of population in the vibro-polariton mode, suggesting a roadmap towards achieving vibro-polariton condensation (in analogy to exciton-polariton condensation [32]) based on the high efficiency of SRS.

We next show how the coexistence of two vibro-polariton modes with similar properties allows to turn the system into an all-optical switch where emission at one frequency is switched by input at another frequency [24, 25]. This is achieved by including a second pump field, with the two pump frequencies chosen to make the Raman process to the two polariton modes $|+\rangle$ and $|-\rangle$ resonant with the same Stokes frequency,

$$\omega_{L\pm} = \omega_S + \omega_\pm, \tag{10}$$

as depicted in Fig. 1(b). Following the procedure of adiabatic elimination and again performing a second RWA to remove terms rotating at frequencies $\pm\Omega_R$ (see [29] for details), we obtain the new effective Hamiltonian

$$\hat{H}^{(2)}_{\rm eff} \simeq \omega_S \hat{n}_S + \sum_{\eta=\{\pm\}} \Big[\omega_{L\eta} \hat{n}_{L\eta} + \omega_\eta \hat{\sigma}_{\eta\eta} - g^\eta_{\rm eff} \left(\hat{\sigma}_{G\eta} \hat{a}_S \hat{a}^\dagger_{L\eta} + {\rm H.c.} \right) \Big], \tag{11}$$

with corresponding Heisenberg-Langevin equations in the mean-field approximation

$$\partial_t \alpha_{L\pm} = i g^\pm_{\rm eff} \psi_\pm \alpha_S - \kappa_L \alpha_{L\pm} + i\sqrt{\kappa_{L\pm}}\Phi^\pm_{\rm in}, \tag{12a}$$
$$\partial_t \alpha_S = i g^+_{\rm eff} \psi_+^* \alpha_{L+} + i g^-_{\rm eff} \psi_-^* \alpha_{L-} - \kappa_S \alpha_S, \tag{12b}$$
$$\partial_t \psi_\pm = i g^\pm_{\rm eff} \alpha_S^* \alpha_{L\pm} - \Gamma_\pm \psi_\pm. \tag{12c}$$

The basic idea for achieving all-optical switching is then to use one of the pump lasers as the input signal ($s = \pm$) and the other pump laser as a gate ($g = \mp$). If the gate beam is turned off, the system is identical to the OPO discussed up to now, and a weak signal beam ($f_s = \Phi^s_{\rm in}/\Phi^s_{\rm th} < 1$) will not lead to lasing, such that the corresponding polaritonic mode is not populated. On the other hand, if the gate beam is strong enough to support OPO operation ($f_g > 1$), the Raman scattering for even a weak signal beam is stimulated by the macroscopic population of the Stokes mode, $|\alpha_S|^2 \gg 1$. We next demonstrate this idea in more detail by solving for the steady state.

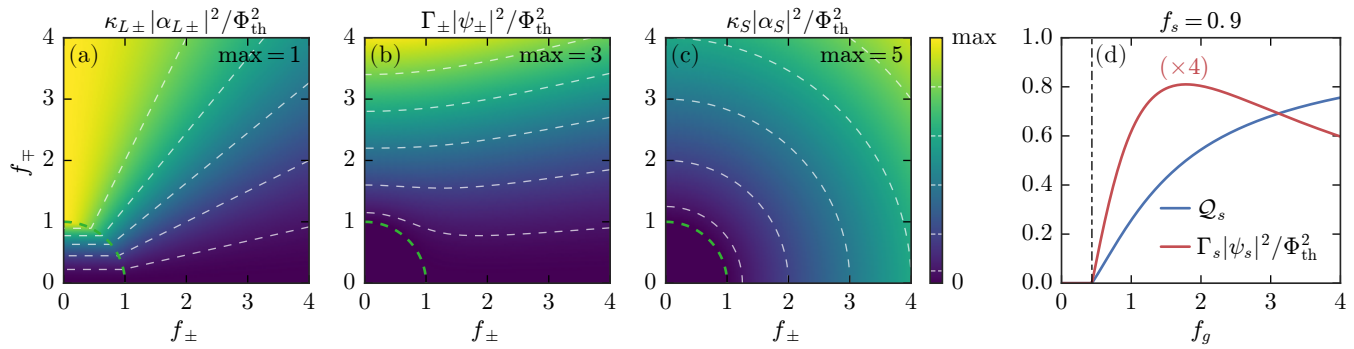

FIG. 2. Rescaled population densities under two-mode pumping with $\Phi_{\rm th}^+ = \Phi_{\rm th}^-$, for (a) the pump mode, (b) the polaritons and (c) the Stokes mode. The green dashed semicircles denote the threshold condition $f_{\rm tot} \geq 1$. (d) Quantum efficiency $\mathcal{Q}_S$ (blue) and rescaled signal polariton density (red, multiplied by 4 for clarity) at a signal pump strength of $f_s = 0.9$ as a function of the gate pump strength f_g.

The relative phases of the different modes are fixed in the steady state, leading to five equations only involving the absolute amplitudes,

$$\kappa_S|\alpha_S| = \sum_{\eta=\{\pm\}} g_{\rm eff}^\eta |\psi_\eta||\alpha_{L\eta}|, \tag{13a}$$

$$\Gamma_\pm|\psi_\pm| = g_{\rm eff}^\pm |\alpha_{L\pm}||\alpha_S|, \tag{13b}$$

$$\kappa_{L\pm}|\alpha_{L\pm}| = \sqrt{\kappa_{L\pm}}\Phi_{\rm in}^\pm - g_{\rm eff}^\pm |\psi_\pm||\alpha_S|. \tag{13c}$$

These equations can be reduced to a quartic polynomial, which permits an analytical solution. The general case is treated in the supplemental material [29], while we here focus on the case that the two thresholds are identical, $\Phi_{\rm th}^+ = \Phi_{\rm th}^- = \Phi_{\rm th}$, which allows for simple analytical expressions. In particular, the threshold condition can then be simplified to $f_{\rm tot} > 1$, where $f_{\rm tot} = \sqrt{f_+^2 + f_-^2}$. Below threshold ($f_{\rm tot} < 1$), the mean-field populations are identical to in the single-pump case, with neither the polariton nor the Stokes modes being populated ($|\psi_\pm|^2 = |\alpha_S|^2 = 0$), while the pump mode populations are just determined by the driving of each mode, $|\alpha_{L\pm}|^2 = f_\pm^2 \Phi_{\rm th}^2/\kappa_L$. Above threshold ($f_{\rm tot} \geq 1$), the Stokes and polariton mode occupations are given by $|\alpha_S|^2 = (f_{\rm tot} - 1)\Phi_{\rm th}^2/\kappa_S$ and $|\psi_\pm|^2 = (f_{\rm tot} - 1)\Phi_{\rm th}^2 f_\pm^2/(f_{\rm tot}^2\Gamma_\pm)$. In contrast to the single-mode OPO case, the pump mode populations are not clamped to a fixed value above threshold, but are given by $|\alpha_{L\pm}|^2 = \Phi_{\rm th}^2 f_\pm^2/(f_{\rm tot}^2\kappa_{L\pm})$. The input power $P_{\rm in}^\pm$ in each pump mode thus does not depend only on the external driving parameter $\Phi_{\rm in}^\pm$, but also on the driving of the other mode $\Phi_{\rm in}^\mp$. The mode populations as a function of f_+ and f_- are shown in Fig. 2. In particular, it should be noted that there is only a single threshold, below which no stimulated emission occurs, and above which all three output modes are populated. Analysis of the fluctuations around the steady-state values demonstrates that the obtained solutions are stable [29]. Thus, *both* polariton modes show stimulated emission due to the population of the Stokes mode as soon as the total pump power becomes large enough. Consequently, the quantum yield for conversion from each pump mode to the corresponding polariton mode, $\mathcal{Q}_\pm = \frac{P_\pm/\omega_\pm}{P_{\rm in}^\pm/\omega_{L\pm}}$, becomes

$$\mathcal{Q}_+ = \mathcal{Q}_- = 1 - \frac{1}{f_{\rm tot}}, \tag{14}$$

where $P_{\rm in}^\pm = \omega_{L\pm}\sqrt{\kappa_{L\pm}}\Phi_{\rm in}^\pm|\alpha_{L\pm}|$ is the input power in pump mode $L\pm$ [29]. In contrast to the "normal" OPO case in Eq. (8), the quantum yield of a given polariton does not depend on the corresponding input power ($\propto f_\pm^2$), but only on the total one ($\propto f_{\rm tot}^2$). This demonstrates that the system can indeed be used like a switch, as sketched above: A below-threshold signal beam input $f_s < 1$ does not produce output in the signal polariton if the gate beam is turned off, but is efficiently converted to signal polaritons if the gate is switched on ($f_g^2 > 1 - f_s^2$). The conversion efficiency of the signal can be made high by making the gate beam sufficiently strong, as demonstrated in Fig. 2(d). The switching speed is limited by the lifetime of the longest-lived state in the system, leading to a tradeoff between achieving low thresholds (requiring small losses) and fast switching speeds (requring large losses).

To conclude, we have demonstrated that by taking advantage of the phenomenon of collective vibrational strong coupling, it is feasible to transform a Raman laser into an OPO. Apart from the improvement of generating two coherent beams both in the visible and in the mid-IR ranges, this new type of OPO presents a lower threshold and less heat generation when compared to a standard Raman laser. Moreover, thanks to the existence of two similar vibro-polaritons, this OPO can also operate as an all-optical switch when excited by two properly designed external beams. Our finding is thus an example of the great potential that hybrid light-matter states possess in both manipulating light fields and modifying material properties.

ACKNOWLEDGMENTS

This work has been funded by the European Research Council (ERC-2011-AdG proposal No. 290981), by the European Union Seventh Framework Programme under grant agreement FP7-PEOPLE-2013-CIG-618229, and the Spanish MINECO under contract MAT2014-53432-C5-5-R and the "María de Maeztu" programme for Units of Excellence in R&D (MDM-2014-0377).

[1] A. Shalabney, J. George, J. Hutchison, G. Pupillo, C. Genet, and T. W. Ebbesen, "Coherent coupling of molecular resonators with a microcavity mode," Nat. Commun. **6**, 5981 (2015).

[2] Jino George, Atef Shalabney, James A. Hutchison, Cyriaque Genet, and Thomas W. Ebbesen, "Liquid-Phase Vibrational Strong Coupling," J. Phys. Chem. Lett. **6**, 1027–1031 (2015).

[3] J. P. Long and B. S. Simpkins, "Coherent Coupling between a Molecular Vibration and Fabry-Perot Optical Cavity to Give Hybridized States in the Strong Coupling Limit," ACS Photonics **2**, 130–136 (2015).

[4] Javier del Pino, Johannes Feist, and Francisco J. Garcia-Vidal, "Quantum theory of collective strong coupling of molecular vibrations with a microcavity mode," New J. Phys. **17**, 053040 (2015).

[5] B. S. Simpkins, Kenan P. Fears, Walter J. Dressick, Bryan T. Spann, Adam D. Dunkelberger, and Jeffrey C Owrutsky, "Spanning Strong to Weak Normal Mode Coupling between Vibrational and Fabry–Pérot Cavity Modes through Tuning of Vibrational Absorption Strength," ACS Photonics **2**, 1460–1467 (2015).

[6] Merav Muallem, Alexander Palatnik, Gilbert D. Nessim, and Yaakov R. Tischler, "Strong Light-Matter Coupling and Hybridization of Molecular Vibrations in a Low-Loss Infrared Microcavity," J. Phys. Chem. Lett. **7**, 2002–2008 (2016).

[7] Atef Shalabney, Jino George, Hidefumi Hiura, James A. Hutchison, Cyriaque Genet, Petra Hellwig, and Thomas W. Ebbesen, "Enhanced Raman Scattering from Vibro-Polariton Hybrid States," Angew. Chemie Int. Ed. **54**, 7971–7975 (2015).

[8] Javier del Pino, Johannes Feist, and F. J. Garcia-Vidal, "Signatures of Vibrational Strong Coupling in Raman Scattering," J. Phys. Chem. C **119**, 29132–29137 (2015).

[9] Artem Strashko and Jonathan Keeling, "Raman scattering with strongly coupled vibron-polaritons," arXiv:1606.08343.

[10] A. Penzkofer, A. Laubereau, and W. Kaiser, "High intensity Raman interactions," Prog. Quantum Electron. **6**, 55–140 (1979).

[11] R. H. Stolen, "Raman Oscillation in Glass Optical Waveguide," Appl. Phys. Lett. **20**, 62 (1972).

[12] H. M. Pask, "The design and operation of solid-state Raman lasers," Prog. Quantum Electron. **27**, 3–56 (2003).

[13] F. Benabid, J. C. Knight, G. Antonopoulos, and P. St. J. Russell, "Stimulated Raman Scattering in Hydrogen-Filled Hollow-Core Photonic Crystal Fiber," Science **298**, 399–402 (2002).

[14] Ozdal Boyraz and Bahram Jalali, "Demonstration of a silicon Raman laser," Opt. Express **12**, 5269 (2004).

[15] Haisheng Rong, Richard Jones, Ansheng Liu, Oded Cohen, Dani Hak, Alexander Fang, and Mario Paniccia, "A continuous-wave Raman silicon laser," Nature **433**, 725–728 (2005).

[16] Haisheng Rong, Shengbo Xu, Ying-Hao Kuo, Vanessa Sih, Oded Cohen, Omri Raday, and Mario Paniccia, "Low-threshold continuous-wave Raman silicon laser," Nat. Phot. **1**, 232–237 (2007).

[17] T. J. Kippenberg, S. M. Spillane, D. K. Armani, and K. J. Vahala, "Ultralow-threshold microcavity Raman laser on a microelectronic chip," Opt. Lett. **29**, 1224 (2004).

[18] J. K. Brasseur, K. S. Repasky, and J. L. Carlsten, "Continuous-wave Raman laser in H(2)." Opt. Lett. **23**, 367–9 (1998).

[19] Robert W. Boyd, *Nonlinear Optics*, 3rd ed. (Elsevier, 2008).

[20] Irina T. Sorokina and Konstantin L. Vodopyanov, eds., *Solid-State Mid-Infrared Laser Sources*, Topics in Applied Physics, Vol. 89 (Springer Berlin Heidelberg, Berlin, Heidelberg, 2003).

[21] D. F. Walls, "Squeezed states of light," Nature **306**, 141–146 (1983).

[22] M. D. Reid and P. D. Drummond, "Quantum correlations of phase in nondegenerate parametric oscillation," Phys. Rev. Lett. **60**, 2731–2733 (1988).

[23] Min Xiao, Ling An Wu, and H. J. Kimble, "Precision measurement beyond the shot-noise limit," Phys. Rev. Lett. **59**, 278–281 (1987).

[24] Hyatt M. Gibbs, *Optical Bistability: Controlling Light with Light*, Quantum Electronics Series (Academic Press, 1985).

[25] Andrew M. C. Dawes, Lucas Illing, Susan M. Clark, and Daniel J. Gauthier, "All-Optical Switching in Rubidium Vapor," Science **308**, 672–674 (2005).

[26] Howard J. Carmichael, *Statistical Methods in Quantum Optics 2: Non-Classical Fields*, Theoretical and Mathematical Physics (Springer Berlin Heidelberg, Berlin, Heidelberg, 2008) p. 542.

[27] E. Brion, L. H. Pedersen, and K. Mølmer, "Adiabatic elimination in a lambda system," J. Phys. A Math. Theor. **40**, 1033–1043 (2007).

[28] Florentin Reiter and Anders S. Sørensen, "Effective operator formalism for open quantum systems," Phys. Rev. A **85**, 032111 (2012).

[29] See Supplemental Material at URL for details on the adiabatic elimination of the electronically excited states, the general solution under double pumping, and the stability analysis.

[30] R. Houdré, R. P. Stanley, and M. Ilegems, "Vacuum-field Rabi splitting in the presence of inhomogeneous broadening: Resolution of a homogeneous linewidth in an inhomogeneously broadened system," Phys. Rev. A **53**, 2711–2715 (1996).

[31] A. Yariv and W. H. Louisell, "5A2 - Theory of the optical parametric oscillator," IEEE J. Quantum Electron. **2**, 418–424 (1966).

[32] J. Kasprzak, M. Richard, S. Kundermann, A. Baas, P. Jeambrun, J. M. J. Keeling, F. M. Marchetti, M. H. Szymańska, R. André, J. L. Staehli, V. Savona, P. B. Littlewood, B. Deveaud, and Le Si Dang, "Bose-Einstein condensation of exciton polaritons," Nature **443**, 409–14 (2006).

Supplemental material

I. DERIVATION OF THE EFFECTIVE HAMILTONIAN

In this section we illustrate the derivation of the OPO Hamiltonian, as given by Eq. (4) in the main text. We also sketch the extension to the case of an all-optical switch with two input beams. We first describe the adiabatic elimination of the electronically excited states in detail. We assume that the detuning $\Delta = \omega_e - \omega_L$ is large compared with the relevant energy scales for the electronic ground states ($|g^{(i)}\rangle$, $|v^{(i)}\rangle$), and that the interaction terms involving electronic excitations in Eq. (2) in the main text are perturbative. In the following, we denote these terms as $\hat{V} = \hat{V}_+ + \hat{V}_+^\dagger$, where $\hat{V}_+$ contains all the terms *creating* electronic excitations, The occupation of the electronically excited states $|e^{(i)}\rangle$ with free evolution Hamiltonian $\hat{H}_e = \omega_e \sum_{i=1}^N \hat{\sigma}_{ee}^{(i)}$ is hence vanishingly small. In particular, this assumption enables to avoid the coupling of different electronically excited states, simplifying the following treatment. In the adiabatic elimination procedure [S1], the density matrix equations are solved by assuming a slow evolution of the lowest-lying states $|g^{(i)}\rangle$, $|v^{(i)}\rangle$ and the optical modes $\hat{a}_S$, $\hat{a}_L$, determined by $\hat{H}_g = \hat{H}_s + \omega_S \hat{n}_S + \omega_L \hat{n}_L$, with $\hat{H}_s$ given in Eq. (1) in the main text. We here ignore contributions originating from the incoherent dynamics within the electronic excited manifold, which could be introduced by means of effective Lindblad terms [S2], but are negligible for large detuning. To perform the adiabatic approximation, we *i)* apply the *rotating-frame* transformation $\hat{U} = e^{-i(\omega_S \hat{n}_S + \omega_L \hat{n}_L)t}$ and *ii)* we work in the eigenbasis of $\hat{H}_s$. The resulting Hamiltonian is

$$\hat{H}' = \hat{H}_s - \frac{1}{2}\hat{V}_+'^\dagger(t) \sum_{f,l} \frac{\omega_e}{\omega_e - \omega_f - \omega_l} \hat{H}_e^{-1} \hat{v}_+^{(l,f)} e^{i\omega_f t}. \tag{S1}$$

Here, $\hat{V}_+'(t)$ has been expanded in terms of its frequency components $f \in (L, S)$, as well as the system eigenstates $l \in (+, -, \{d\})$ that it couples to, giving

$$\hat{V}_+'(t) = \sum_{f,l} \hat{v}_+^{(f,l)} e^{i\omega_f t} = \sum_{i=1}^N \Bigg[g_L \hat{a}_L \hat{\sigma}_{Ge}^{\dagger(i)} e^{i\omega_L t} + g_S \hat{a}_S \left(\sum_{\eta=\{\pm\}} \frac{\hat{\sigma}_{\eta e}^{\dagger(i)}}{\sqrt{2N}} + \sum_d u_{id} \hat{\sigma}_{de}^{\dagger(i)} \right) e^{i\omega_S t} \Bigg]. \tag{S2}$$

Here, $\hat{\sigma}_{le}^{(i)} = |l\rangle\langle e^i|$, and the coefficients appearing between parenthesis follow from the eigenstate expansions $|v^{(i)}\rangle = (2N)^{-\frac{1}{2}} \sum_{\eta=\{\pm\}} |\eta\rangle + \sum_d u_{id} |d\rangle$, where u_{id} is the overlap matrix element between the ith vibrational excitation and dark state d. These coefficients fulfill $\sum_{i=1}^N u_{id} = 0$ and are further constrained by the orthogonality relation $\sum_{i=1}^N u_{di} u_{id'} = \delta_{dd'}$. After going back to the nonrotating frame, the resulting effective interaction reads

$$\hat{H}_{\text{int}}^{\text{eff}} = -\sum_{\eta=\{\pm\}} g_{\text{eff}}^\eta (\hat{a}_L \hat{a}_S^\dagger \hat{\sigma}_{G\eta}^\dagger + \text{H.c.}), \tag{S3}$$

with $g_{\text{eff}}^\eta = \frac{g_S g_L}{2} \sqrt{\frac{N}{2}} \left[(\omega_e - (\omega_\eta + \omega_S))^{-1} + \Delta^{-1} \right]$. Note here that the contribution of the dark states is identically zero in the effective dynamics. This is due to the fact that we assumed perfect overlap between the involved modes, i.e., we took g, g_S, and g_L to be constant for all involved molecules. Relaxing this condition would give an additional overlap prefactor $g_{\text{eff}}^\eta \to \mathcal{S} g_{\text{eff}}^\eta$, with $\mathcal{S} \propto \sum_i u_{i\eta} g_{S,i} g_{L,i}^*$, and also give nonzero coupling to the dark states, but would not otherwise change the results presented in the main text. In addition to the effective interaction, we obtain (nonlinear) energy shifts, given by

$$\hat{H}_{\text{shift}}^{\text{eff}} = -\frac{g_L^2 N}{\Delta} \hat{n}_L \hat{\sigma}_{GG} - \sum_l \frac{g_S^2 \hat{n}_S \hat{\sigma}_{ll}}{\omega_e - (\omega_l + \omega_S)}. \tag{S4}$$

Under the assumption that the output modes are not significantly populated ($\hat{\sigma}_{GG} \approx 1$, $\hat{n}_S, \hat{\sigma}_{\eta\eta} \ll 1$), the first term just gives a constant energy shift (which we assume to be included into ω_L), while the second term can be neglected. This is a good approximation for typical system parameters even when a large number of output photons is generated, due to the relatively short lifetime of the polaritons. Under this approximation, the vibropolaritons are well-modeled as bosons $[\hat{\sigma}_{G\eta}, \hat{\sigma}_{G\eta'}^\dagger] \simeq \delta_{\eta\eta'}$, and the trilinear interaction Eq. (S5) corresponds to a nondegenerate OPO under the identifications $\hat{a}_S \to$ signal, $\hat{\sigma}_{Gp} \to$ idler.

For a laser frequency chosen such that Raman scattering to one of the polaritonic modes is resonant with the cavity mode S in the optical, $\omega_L = \omega_S + \omega_p$, with $p \in \{\pm\}$, there are rapidly oscillating terms in Eq. (S3) in the interaction picture with regards to $\hat{H}_g$. Averaging over a time sufficiently big compared to $\tau_{\text{coh}} \sim \Omega_R^{-1}$, these contributions, which correspond to the coupling of the laser field with the detuned polariton, can be neglected under a *second* rotating wave approximation, giving

$$\hat{H}_{\text{eff}} \simeq \omega_L \hat{n}_L + \omega_S \hat{n}_S + \omega_p \hat{\sigma}_{pp} - g_{\text{eff}}^p \left(\hat{a}_L \hat{a}_S^\dagger \hat{\sigma}_{Gp}^\dagger + \text{H.c.} \right). \tag{S5}$$

We next sketch the derivation of the effective Hamiltonian under pumping of multiple input modes, as given by Eq. (11) in the main text. The pumping Hamiltonian is then

$$\hat{H}_d^{(2)} = \sum_{\eta=\{\pm\}} \sqrt{\kappa_{L\eta}} \Phi_{\text{in}}^\eta (\hat{a}_{L\eta} e^{-i\omega_{L\eta} t} + \hat{a}_{L\eta}^\dagger e^{i\omega_{L\eta} t}), \tag{S6}$$

while the pump-system interaction is given by

$$\hat{V}_+ = \sum_{i=1}^{N} \left(g_S \hat{a}_S \hat{\sigma}^\dagger_{v_i e_i} + \sum_{\eta=\{\pm\}} g_{L\eta} \hat{a}_{L\eta} \hat{\sigma}^\dagger_{g_i e_i} \right). \tag{S7}$$

The frequencies $\omega_{L\pm}$ are chosen to satisfy the resonance conditions for both polaritons, $\omega_{L\pm} = \omega_S + \omega_\pm$. The adiabatic elimination of the electronic states proceeds analogously to the single-pump case, giving the effective interaction Hamiltonian

$$\hat{H}^{\mathrm{eff}(2)}_{\mathrm{int}} = - \sum_{\eta,\eta'=\{\pm\}} g^{\eta,\eta'}_{\mathrm{eff}} (\hat{a}_{L\eta'} \hat{a}^\dagger_S \hat{\sigma}^\dagger_{G\eta} + \mathrm{H.c.}), \tag{S8}$$

where the effective coupling constant of the pump field η with the polariton η' is (using $\Delta_\pm = \omega_e - \omega_{L\pm}$)

$$g^{\eta,\eta'}_{\mathrm{eff}} = \frac{g_S g_{L\eta}}{2} \sqrt{\frac{N}{2}} \left[\frac{1}{\omega_e - (\omega_{\eta'} + \omega_S)} + \frac{1}{\Delta_\eta} \right]. \tag{S9}$$

The off-diagonal terms $\eta \neq \eta'$ can be neglected under the same *second* RWA we invoked for the OPO case. In addition to the effective interaction, we again obtain extra nonlinear terms, given by

$$\hat{H}^{\mathrm{eff}(2)}_{\mathrm{extra}} = - \sum_{\eta,\eta'} \Lambda^{\eta,\eta'}_{\mathrm{eff}} \hat{\sigma}_{GG} (\hat{a}^\dagger_{L\eta} \hat{a}_{L\eta'} + \mathrm{H.c.}) - \hat{n}_S \sum_l \frac{g_S^2 \hat{\sigma}_{ll}}{\omega_e - (\omega_l + \omega_S)}, \tag{S10}$$

which in addition to the energy shifts already seen in the single-pump OPO case also contains an extra crossed term coupling the two pump fields. The nonlinear terms Eq. (S10) can again be neglected under the low-occupation assumption and the second RWA. Finally, we thus obtain

$$\hat{H}^{(2)}_{\mathrm{eff}} \simeq \omega_S \hat{n}_S + \sum_{\eta=\{\pm\}} \Big[\omega_{L\eta} \hat{n}_{L\eta} + \omega_\eta \hat{\sigma}_{\eta\eta} - g^\eta_{\mathrm{eff}} (\hat{\sigma}_{G\eta} \hat{a}_S \hat{a}^\dagger_{L\eta} + \mathrm{H.c.}) \Big], \tag{S11}$$

where we used that $g^{\eta,\eta}_{\mathrm{eff}} = g^\eta_{\mathrm{eff}}$.

II. MEAN-FIELD STEADY-STATE SOLUTIONS

We here discuss the general steady-state solution for the optical-switch setup with multiple pump beams. For clarity, we first recall the well-known Manley-Rowe relations for beam fluxes and powers [S3] in the single-pump case, which follow straightforwardly from the semiclassical equations Eq. (7) in the main text. They connect the fluxes of emitted photons $P_i/\omega_i = \gamma_i |\alpha_i|^2$ in the different modes, with the simple relation

$$\frac{P_S}{\omega_S} = \frac{P_p}{\omega_p} = \frac{P^{\mathrm{th}}_L}{\omega_L} (f - 1), \qquad f = \frac{\Phi_{\mathrm{in}}}{\Phi_{\mathrm{th}}}. \tag{S12}$$

This explicitly shows that Raman scattering converts each of the incoming pump photons into a Stokes photon/polariton pair. From Eq. (S12) and the resonance condition $\omega_L = \omega_S + \omega_p$, we obtain the power relation $P_{\mathrm{in}} = P_S + P_p + P^{\mathrm{th}}_L$. This expresses the fact that the input power $P_{\mathrm{in}} = \omega_L \Phi_{\mathrm{in}} \Phi_{\mathrm{th}}$ is shared among the three modes, with a maximum clamped power for the L mode at threshold equal to Φ^2_{th}. From the analogue steady-state relations within the two-pump scenario, a set of generalized Manley-Rowe relations accounting for the exchange of energy between the modes participating in the scattering holds:

$$\frac{P_S}{\omega_S} = \sum_{\eta=\{\pm\}} \frac{P_\eta}{\omega_\eta}, \qquad \frac{P_\pm}{\omega_\pm} = \frac{P^\pm_{\mathrm{in}} - P_{L\pm}}{\omega_{L\pm}}, \tag{S13}$$

where the input power in each of the pump modes $L\pm$ is $P^\pm_{\mathrm{in}} = \omega_{L\pm} \sqrt{\kappa_{L\pm}} \Phi^\pm_{\mathrm{in}} |\alpha_{L\pm}|$. Employing the resonance conditions for the two pumps, we obtain the global power relation $\sum_{\eta=\{\pm\}} P^\eta_{\mathrm{in}} = P_S + \sum_{\eta=\{\pm\}} (P_\eta + P_{L\eta})$, a direct generalization of Eq. (S12).

We now proceed to solve the steady-state equations, Eq. (13) in the main text, under pumping of both modes ($\Phi^\pm_{\mathrm{in}} > 0$). The following relations between the $L\pm$ amplitudes hold,

$$\frac{\kappa_{L+} |\alpha_{L+}|^2}{\Phi^{+2}_{\mathrm{th}}} + \frac{\kappa_{L-} |\alpha_{L-}|^2}{\Phi^{-2}_{\mathrm{th}}} = 1, \tag{S14}$$

expressing the fact that the *global* pump amplitude becomes clamped above the threshold due to its connection to a common Stokes mode (with $\Phi^\pm_{\mathrm{th}} = \sqrt{\kappa_{L\pm} \kappa_S \Gamma_\pm} / g^\pm_{\mathrm{eff}}$). As we will see in the following, this is not the case for each of the pumping amplitudes individually. The relation Eq. (S14) suggests we can define

$$|\alpha_{L+}| = \frac{\Phi^+_{\mathrm{th}}}{\sqrt{\kappa_{L+}}} \sin\Theta, \quad |\alpha_{L-}| = \frac{\Phi^-_{\mathrm{th}}}{\sqrt{\kappa_{L-}}} \cos\Theta, \tag{S15}$$

with mixing angle Θ in the range $\Theta \in (0, \pi/2)$, such that $|\alpha_{L\pm}| > 0$. Inserting this into the steady state-equations leads to a quartic equation for $t = \tan(\Theta/2)$, given by

$$t^4 + 2(\alpha - \beta) t^3 + 2(\alpha + \beta) t - 1 = 0, \tag{S16}$$

where $\alpha = \Phi^-_{\mathrm{in}} \Phi^-_{\mathrm{th}} / (\Phi^+_{\mathrm{in}} \Phi^+_{\mathrm{th}})$, and $\beta = [(\Phi^+_{\mathrm{th}})^2 - (\Phi^-_{\mathrm{th}})^2] / (\Phi^+_{\mathrm{in}} \Phi^+_{\mathrm{th}})$. We have checked that this equation has only one physical solution $0 < t < 1$ for arbitrary values of $\alpha > 0$) and β. The analytical form of the solution of Eq. (S16) is very lengthy and we thus omit it in the following. However, in the degenerate case with equal thresholds, we get $\beta = 0$ and the equation can be factorized as $\left(t^2 + 1\right)\left(t^2 + 2\alpha t - 1\right) = 0$, leading to the single physical solution analyzed in the main text, $t = \sqrt{1 + \alpha^2} - \alpha$, with $\alpha = f_-/f_+$.

III. STABILITY OF THE MEAN-FIELD SOLUTIONS

We here analyze the stability of the semiclassical steady-state solutions of Eq. (12) in the main text. Collecting these solutions in the vector $\boldsymbol{v}^\infty = (\alpha_S, \psi_+, \alpha_{L+}, \psi_-, \alpha_{L-}, \text{H.c.})$, inserting the linearized solution $\boldsymbol{v}(t) = \boldsymbol{v}^\infty + \delta\boldsymbol{v}(t)$ in Eq. (12) and keeping terms $O(\delta\boldsymbol{v})$, we obtain the time evolution of the fluctuations, $\partial_t \delta\boldsymbol{v}(t) = \boldsymbol{\mathcal{M}}\delta\boldsymbol{v}(t)$. The stability matrix is

$$\boldsymbol{\mathcal{M}} = \left(\begin{array}{c|cc} -\kappa_S \mathbb{1}_{2\times 2} & \boldsymbol{v}_+ & \boldsymbol{v}_- \\ \hline \boldsymbol{u}_+^T & -\boldsymbol{\mathcal{P}}_+ & 0 \\ \boldsymbol{u}_-^T & 0 & -\boldsymbol{\mathcal{P}}_- \end{array}\right), \tag{S17}$$

where the submatrices are

$$\boldsymbol{v}_\pm = i g_{\text{eff}}^\pm \begin{pmatrix} 0 & \alpha_{L\pm} & \psi_\pm^* & 0 \\ -\alpha_{L\pm}^* & 0 & 0 & -\psi_\pm \end{pmatrix}, \tag{S18a}$$

$$\boldsymbol{u}_\pm = i g_{\text{eff}}^\pm \begin{pmatrix} \alpha_{L\pm} & 0 & 0 & -\psi_\pm^* \\ 0 & -\alpha_{L\pm}^* & \psi_\pm & 0 \end{pmatrix}, \tag{S18b}$$

$$\boldsymbol{\mathcal{P}}_\pm = \begin{pmatrix} \Gamma_\pm & 0 & -i g_{\text{eff}}^\pm \alpha_S^* & 0 \\ 0 & \Gamma_\pm & 0 & i g_{\text{eff}}^\pm \alpha_S \\ -i g_{\text{eff}}^\pm \alpha_S & 0 & \kappa_{L\pm} & 0 \\ 0 & i g_{\text{eff}}^\pm \alpha_S^* & 0 & \kappa_{L\pm} \end{pmatrix}. \tag{S18c}$$

The fluctuations $\delta\boldsymbol{v}(t)$ will grow exponentially in time if the real part of any eigenvalue of $\boldsymbol{\mathcal{M}}$ is positive. This can be tested via the Routh-Huwirtz criterion [S4], which provides necessary and sufficient conditions for the roots of the characteristic polynomial $\det\left(\boldsymbol{\mathcal{M}} - \lambda \mathbb{1}_{10\times 10}\right)$ to have negative real part, without explicit knowledge of their values. Applying this criterion proves that the all-optical switch solutions pictured in the main text are stable. From this, the stability of the OPO solutions under single-mode driving follows automatically.

[S1] Herman Feshbach, "Unified theory of nuclear reactions," Ann. Phys. (N. Y.). **5**, 357–390 (1958).

[S2] Florentin Reiter and Anders S. Sørensen, "Effective operator formalism for open quantum systems," Phys. Rev. A **85**, 032111 (2012).

[S3] A. Yariv and W. H. Louisell, "5A2 - Theory of the optical parametric oscillator," IEEE J. Quantum Electron. **2**, 418–424 (1966).

[S4] Izrail Solomonovich Gradshteyn and Iosif Moiseevich Ryzhik, *Table of integrals, series, and products*, eigth ed., edited by Daniel Zwillinger (Elsevier, 2014).